

the presence of  $P_i$  can be explained by reversal of reactions 5 and 4. A reversible attachment step was also included in our recently published kinetic simulation (10) for two reasons: (i) it allows for current estimates of the number of cross-bridges attached during active contraction and (ii) it explains the observation that the final relaxation rate after caged ATP photolysis (Fig. 1B) is more rapid than the overall rate of ATP hydrolysis per myosin head ( $<2 \text{ sec}^{-1}$ ) (16).

If attachment and force generation are indeed reversible, then the observed rate constant for tension redevelopment in the presence of  $\text{Ca}^{2+}$  would be given by the sum of the forward and reverse reaction rates. An increase in  $P_i$  concentration would then increase the rate constant for tension redevelopment by increasing the rate of reversal of reaction 5 and would decrease steady active tension by shifting the distribution of cross-bridge states toward  $\text{AM} \cdot \text{ADP} \cdot P_i$  and  $\text{M} \cdot \text{ADP} \cdot P_i$ .

Our interpretation is based on the assumption that the mechanical measurements reflect  $P_i$  binding to the myosin active site (reversal of reaction 5). Alternatively,  $P_i$  might increase the rate of the forward reactions 6 and 7. This seems unlikely, however, because the rate of ATP hydrolysis by an actively contracting fiber would then be expected to increase markedly in the presence of  $P_i$ . However, other effects of  $P_i$  on reactions 6 and 7 have not been ruled out.

Addition of ADP and then  $P_i$  to a muscle fiber in the rigor state does not decrease the tension. Thus the results of our photolysis experiments suggest that  $P_i$  binds to the  $\text{AM}' \cdot \text{ADP}$  formed only through reactions 3, 4, and 5 during ATP hydrolysis, as proposed for isolated actomyosin (17). The lifetime of  $\text{AM}' \cdot \text{ADP}$  has not been quantitatively determined in isolated actomyosin or in fibers. However, mechanical strain on the cross-bridge might shift the equilibrium between  $\text{AM}' \cdot \text{ADP}$  and  $\text{AM} \cdot \text{ADP} \cdot P_i$  toward  $\text{AM} \cdot \text{ADP} \cdot P_i$ . In that case  $\text{AM}' \cdot \text{ADP}$  would produce more mechanical force than  $\text{AM} \cdot \text{ADP} \cdot P_i$  and the hypothesis would imply that  $P_i$  release is intimately coupled to formation of the dominant force-generating state (18).

Our results may help to explain other mechanical phenomena in muscles. Inorganic phosphate reduces the amplitude of stretch-induced activation in insect fibrillar flight muscle (19) and increases the relaxation rate of skinned smooth muscle (20). These effects are consistent with a reversal of step 5, although other factors may be involved. During fatigue

of intact vertebrate skeletal muscle, tension decreases as  $P_i$ , ADP, and  $\text{H}^+$  concentrations increase (1). If the accumulation of  $P_i$  contributes to this decrease in tension (21), then our results provide a qualitative explanation for fatigue development in terms of cross-bridge kinetics.

MARK G. HIBBERD  
JODY A. DANTZIG

Department of Physiology,  
University of Pennsylvania School of  
Medicine, Philadelphia 19104

DAVID R. TRENTHAM  
National Institute for Medical  
Research, London, NW7 1AA, England

YALE E. GOLDMAN  
Department of Physiology, University  
of Pennsylvania School of Medicine

#### References and Notes

1. M. J. Dawson, D. G. Gadian, D. R. Wilkie, *Nature (London)* **274**, 861 (1978).
2. J. W. Herzig and J. C. Rüegg, in *Myocardial Failure*, G. Riecker, Ed. (Springer-Verlag, Berlin, 1977), pp. 41–51.
3. P. W. Brandt *et al.*, *J. Gen. Physiol.* **79**, 997 (1982).
4. J. H. Kaplan, B. Forbush III, J. F. Hoffman, *Biochemistry* **17**, 1929 (1978).
5. Y. E. Goldman, M. G. Hibberd, D. R. Trentham, *J. Physiol. (London)* **354**, 577 (1984).
6. Y. E. Goldman *et al.*, *Nature (London)* **300**, 701 (1982).
7. A. F. Huxley and R. M. Simmons, *ibid.* **233**, 533 (1971).
8. Y. E. Goldman and R. M. Simmons, *J. Physiol. (London)* **269**, 55P (1977).
9. M. Kawai and P. W. Brandt, *J. Muscle Res. Cell Motil.* **1**, 279 (1980).
10. Y. E. Goldman, M. G. Hibberd, D. R. Trentham, *J. Physiol. (London)* **354**, 605 (1984).
11. E. W. Taylor, *CRC Crit. Rev. Biochem.* **6**, 103 (1979).
12. E. Eisenberg and L. E. Greene, *Annu. Rev. Physiol.* **42**, 293 (1980).
13. R. W. Lyman and E. W. Taylor, *Biochemistry* **10**, 4617 (1971).
14. D. Mornet *et al.*, *Nature (London)* **292**, 301 (1981).
15. J. A. Sleep and R. L. Hutton, *Biochemistry* **17**, 5423 (1978).
16. M. A. Ferenczi, E. Homsher, D. R. Trentham, *J. Physiol.* **352**, 575 (1984).
17. J. A. Sleep and R. L. Hutton, *Biochemistry* **19**, 1276 (1980).
18. A. F. Huxley, *Reflections on Muscle* (Princeton Univ. Press, Princeton, N.J., 1980), pp. 93–95.
19. D. C. S. White and J. Thorson, *J. Gen. Physiol.* **60**, 307 (1972).
20. K. Güth and J. Junge, *Nature (London)* **300**, 775 (1982).
21. R. E. Godt *et al.*, paper presented at the Eighth International Biophysics Congress, Bristol, England (1984).
22. Supported by NIH grant HL15835 to the Pennsylvania Muscle Institute, NIH grant AM00745, and the Muscular Dystrophy Associations of America. M.G.H. was a British-American Heart Fellow.

27 November 1984; accepted 8 February 1985

## Defect in Vitamin B<sub>12</sub> Release from Lysosomes: Newly Described Inborn Error of Vitamin B<sub>12</sub> Metabolism

**Abstract.** *Cultured diploid fibroblasts from a patient with a previously undescribed inborn error of cobalamin metabolism accumulate unmetabolized, nonprotein-bound vitamin B<sub>12</sub> in lysosomes. These cells are able to endocytose the transcobalamin II-B<sub>12</sub> complex and to release B<sub>12</sub> from transcobalamin II. The freed vitamin B<sub>12</sub> is not released from lysosomes into the cytoplasm of the cell. This suggests that there is a specific lysosomal transport mechanism for vitamin B<sub>12</sub> in the human.*

Vitamin B<sub>12</sub> (cobalamin) coenzymes in mammalian cells mediate three apoenzyme-catalyzed reactions in mammalian cells: (i) synthesis of methionine from homocysteine, which is mediated by methyl cobalamin ( $\text{CH}_3\text{-B}_{12}$ ); (ii) interconversion of methylmalonyl coenzyme A and succinyl coenzyme A; (iii) and interconversion of  $\alpha$ - and  $\beta$ -leucine. The latter two reactions are mediated by 5' deoxyadenosyl cobalamin (Ado-B<sub>12</sub>). The importance in human metabolism of the first two reactions has been revealed by inherited defects in these reactions; cells from patients with vitamin B<sub>12</sub>-responsive forms of these disorders are defective in accumulation of the appropriate coenzyme form of cobalamin (1). The entry of physiological concentrations of cobalamin into mammalian cells is dependent on the presence of a transport protein that binds the cobalamin [transcobalamin II (TCII)]; interaction of the protein-cobalamin complex with specific receptors on the cell surface; endo-

cytosis of the complex; degradation of the binding protein by lysosomal proteases; and release of the free vitamin B<sub>12</sub> into the cytoplasm (2). Although a complex transport system for the entry of vitamin B<sub>12</sub> into bacteria and several mutants has been described (3), the only inherited defect reported to affect the entry of cobalamin into mammalian cells is the absence of biologically active TCII. We now describe a defect in the transport of cobalamin from lysosome to cytoplasm.

Skin fibroblasts were obtained from an infant girl with developmental delay, minimal methylmalonic aciduria (50 mg/100 ml) responsive to vitamin B<sub>12</sub>, and no megaloblastic anemia or homocystinuria. Control and proband fibroblasts, free from mycoplasma contamination, were grown in Eagle's minimum essential medium containing 10 percent fetal bovine serum. Cobalamin uptake was studied by replacing the fetal bovine serum with 10 percent human serum

Table 1. Subcellular localization of cobalamin in fibroblasts from the patient and from control cells. Cultured fibroblasts were incubated in medium containing [<sup>57</sup>Co]CN-B<sub>12</sub> (25 pg/ml) and 10 percent human serum for 24 hours (4). The cells were harvested with 0.25 percent trypsin and washed three times with phosphate-buffered saline (pH 7.4). The final pellet was suspended in 0.6 ml of cold 0.25M sucrose to which was added 250 USP units of heparin (10,000 USP unit/ml) (7, 8). Incubation was carried out for 20 minutes on ice. Aliquots (20 μl) were taken to monitor the dissolution of cell membranes. After heparin treatment, the sample (0.5 ml) was layered on 9.9 ml of cold isosmotic (0.25M sucrose) Percoll at a density of 1.09 g/ml in a 10.4-ml Beckman Polycarbonate tube and then centrifuged for 120 minutes at 65,000g. After centrifugation, 20 fractions of 0.5 ml were collected from the bottom of the tube. Aliquots were taken for radioactivity and lysosomal markers.

| Fractions | Density        | Lysosomal markers<br>(percent of total activity) |                            | [ <sup>57</sup> Co]CN-B <sub>12</sub> uptake<br>(percent of total activity) |         |
|-----------|----------------|--|----------------------------|---|---------|
|           |                | Acid phosphatase                                 | N-Acetyl-β-glucosaminidase | Control   | Patient |
| 1 to 14   | 1.036 to 1.096 | 90.3   | 89.6                       | 37.5  | 92.8    |
| 15 to 20  | <1.036         | 9.7  | 10.4                       | 62.5  | 7.2     |

previously incubated with [<sup>57</sup>Co]cyanocobalamin (CN-B<sub>12</sub>). Separation of bound and free cobalamin extracted from the cells was determined by filtration of cell extracts through Sephadryl S-200 (4). Intracellular cobalamins were fractionated by extraction in hot ethanol followed by high-performance liquid chromatography (4).

Confluent cultured fibroblasts from the patient were grown in medium containing labeled CN-B<sub>12</sub> (25 pg/ml). After 4 days of incubation, the patient's fibroblasts accumulated higher total intracellular concentrations of labeled cobalamin (52 pg per milligram of protein) than did control cells at the same stage of

growth (16 pg/mg) and much more than did cobalamin C (4 pg/mg) or cobalamin D (6 pg/mg) mutant fibroblasts (1), which are defective in cobalamin accumulation. The labeled cobalamin in extracts of the patient's cells was more than 90 percent CN-B<sub>12</sub>, whereas in control cells it was 2 to 5 percent CN-B<sub>12</sub>, 50 percent CH<sub>3</sub>-B<sub>12</sub>, and 15 percent Ado-B<sub>12</sub>. Gel filtration of cell homogenates on Sephadryl S-200 after the cells were grown in CN-B<sub>12</sub> at either 25 or 250 pg/ml revealed that more than 95 percent of the label in control cells was associated with macromolecules (previously shown to be cobalamin-dependent enzymes), whereas most of the label in the patient's cells

was associated with free cobalamin (Fig. 1).

When cell extracts were applied to a Percoll gradient to separate cytoplasmic from mitochondrial and lysosomal material, most of the label in the control cells was in the lowest density (cytoplasmic) fraction, whereas most of the label in the patient's cells was in the particulate fraction (Table 1).

The effect of intralysosomal digestion on cobalamin in these cells was determined by incubating fibroblasts in cobalamin (250 pg/ml) and human serum, to which was added 25 μM chloroquine. Chloroquine accumulates in lysosomes and retards intralysosomal proteolysis. Filtration of cell extract through Sephadryl S-200 revealed (Fig. 1) that, in both the patient's and control cells, most of the cobalamin filtered at a molecular weight of about 40,000, which is the size of TCII-B<sub>12</sub>. These studies show that vitamin B<sub>12</sub> bound to TCII is able to enter the lysosomes of the patient's cells in the same manner as it enters into control cells.

Like control cells, fibroblasts from our patient accumulated TCII-B<sub>12</sub> within lysosomes and released the vitamin from the binding protein. The patient's cells are defective in the transfer of intralysosomal cobalamin into the cytoplasm. The defect appears to be analogous to the one observed in the cells of patients with cystinosis in which cystine accumulates in lysosomes (5, 6). Fibroblasts from our patient contained 0.35 μmol of half-cystine per gram of protein as compared to 5.0 μmol per gram of protein in fibroblasts from a patient with cystinosis. Unlike the finding in cystinosis, no abnormal lysosomal structures were observed in these fibroblasts on examination by electron microscopy. We suggest that our patient has a defect in a transport system required for the transmembrane transfer of cobalamin from lysosomes into cytoplasm and that such a system exists in mammalian cells.

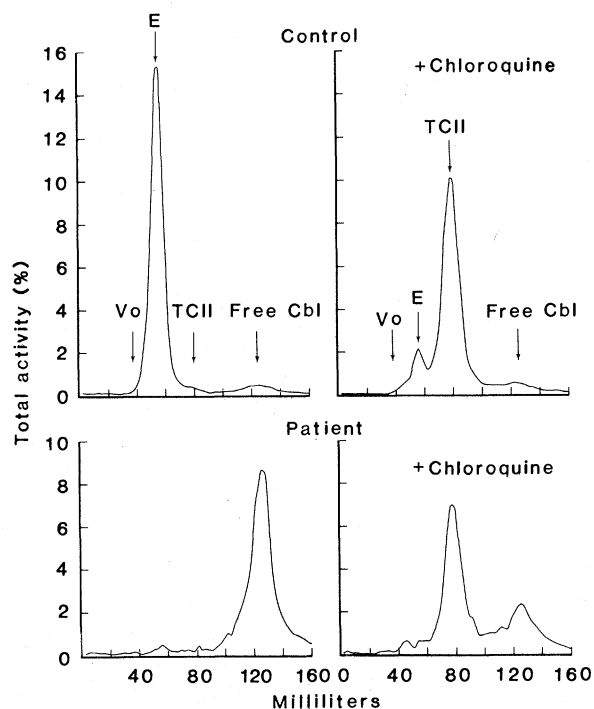
DAVID S. ROSENBLATT\*  
ANGELA HOSACK  
NORA V. MATIASZUK

Centre for Human Genetics, Medical Research Council of Canada Genetics Group, and Departments of Pediatrics and Biology, McGill University, Montreal, Quebec H3H 1P3, Canada

BERNARD A. COOPER  
Departments of Physiology and Medicine, McGill University

RACHEL LAFRAMBOISE  
Réseau de Médecine Génétique du Québec, Le Centre Hospitalier de l'Université Laval, Québec

Fig. 1. Sephadryl S-200 elution pattern of <sup>57</sup>Co in fibroblast extracts. Control cells and fibroblasts from the patient were incubated in Eagle's minimum essential medium plus nonessential amino acids. (Left) The cells were incubated in [<sup>57</sup>Co]CN-B<sub>12</sub> (250 pg/ml) in 10 percent human serum for 20 hours. (Right) Replicate cultures were incubated in medium containing 25 μM chloroquine for 1 hour before being incubated for 20 hours in medium containing labeled B<sub>12</sub> and chloroquine. After the cells were harvested with trypsin, they were suspended in 0.1M potassium phosphate (pH 7.4), sonicated on ice, and centrifuged for 60 minutes at 27,000g. The supernatant was applied to a Sephadryl S-200 Superfine column (1.6 by 66 cm) and eluted with the same buffer; 2-ml fractions were collected and <sup>57</sup>Co activity was determined. Vo indicates the void volume; E, the position of both methionine synthase and methylmalonyl-coenzyme A mutase, which elute as a single peak (4); TCII, the position of transcobalamin II; and free Cbl, the position of B<sub>12</sub> which is not protein-bound within the cell.



## References and Notes

1. L. E. Rosenberg in *The Metabolic Basis of Inherited Disease*, J. B. Stanbury et al., Eds. (McGraw-Hill, New York, 1983), p. 474.
2. P. Youngdahl-Turner and L. E. Rosenberg, *J. Clin. Invest.* **61**, 133 (1978).
3. C. Bradbeer, in *Vitamin B<sub>12</sub>*, B. Zagalak and W. Friedrich, Eds. (de Gruyter, New York, 1979), p. 711.
4. D. S. Rosenblatt, B. A. Cooper, A. Pottier, H. Lue-Shing, N. Matiaszuk, K. Grauer, *J. Clin. Invest.* **74**, 2149 (1984).
5. W. A. Gahl et al., *Science* **217**, 1263 (1982).
6. W. A. Gahl et al., *J. Biol. Chem.* **257**, 9570 (1982).
7. A. Dubin, A. Koj, J. Chudzick, *Biochem. J.* **153**, 389 (1976).
8. W. B. Chodirker, G. N. Bock, J. H. Vaughan, *J. Lab. Clin. Med.* **71**, 9 (1968).
9. This is publication 85007 from the McGill University Montreal Children's Hospital Research Institute.

\* To whom requests for reprints should be sent at 2300 Tupper Street, A709 Montreal, Quebec H3H 1P3, Canada.

26 December 1984; accepted 22 February 1985

## Correlated Measurements of DNA, RNA, and Protein in Individual Cells by Flow Cytometry

**Abstract.** A cytochemical method was developed to differentially stain cellular DNA, RNA, and proteins with fluorochromes Hoechst 33342, pyronin Y, and fluorescein isothiocyanate, respectively. The fluorescence intensities, reflecting the DNA, RNA, and protein content of individual cells, were measured in a flow cytometer after sequential excitation by three lasers tuned to different excitation wavelengths. The method offers rapid analysis of changes in the cellular content of RNA and protein as well as in the RNA-protein, RNA-DNA, and protein-DNA ratios in relation to cell cycle position for large cell populations. An analysis of cycling cell populations (exponentially growing CHO cultures) and noncycling CHO cells arrested in the G<sub>1</sub> phase by growth in isoleucine-free medium demonstrated the potential of the technique.

Flow cytometric analysis of DNA content in single cells provides a rapid and accurate method for determining the cell cycle frequency distribution of a given population (1). Determinations based on DNA content alone, however, cannot discriminate among the many metabolic states related to a cell's capacity to progress through the cell cycle. Distinctions between quiescent and cycling cells or among cells in various stages of differentiation, and the relation between cell growth and DNA division, can be better assessed by multiparametric analysis of DNA and RNA (2) or DNA and protein (3). For instance, in certain cell systems quiescent (G<sub>0</sub>, G<sub>1</sub>Q) or differentiating (G<sub>1</sub>D) cells can be distinguished from cycling G<sub>1</sub> cells on the basis of RNA content (4). In other systems some cells may be characterized by an S-phase DNA content but may not traverse the S phase or traverse it very slowly; such cells (S<sub>Q</sub>) can also be recognized by multiparametric analysis (4). A critical RNA content and, perhaps, also a protein content for cells in G<sub>1</sub> discriminates between two functionally distinct compartments of G<sub>1</sub>, G<sub>1</sub>A and G<sub>1</sub>B, believed to have different roles in the cell cycle (5). To our knowledge, a method has not been found to measure simultaneously DNA, RNA, and protein in the same cells. Such measurements, especially when combined with an assessment of the ratio of RNA to DNA or RNA to protein per cell, can provide additional information on cell metabolism as relat-

ed to cell cycle, quiescence, differentiation, transformation, or sensitivity to drug treatment, and may offer a new method for recognizing and classifying tumor cells.

We report here a flow cytometric method for the direct determination and

correlation of DNA, RNA, and protein content in individual cells (6). The cytochemical reaction incorporates modified procedures for staining DNA with Hoechst 33342 (7), RNA with pyronin Y (PY) (8), and protein with fluorescein isothiocyanate (FITC) (3). Stained cells are analyzed with a three-laser excitation flow system (9).

One of the main difficulties in multicolor fluorescence analysis arises from the overlap in the fluorescence excitation and emission spectra of the individual dyes. With spatially separated laser beams, each set at a wavelength near the optimum for excitation of a given dye and appropriate filter arrangements, we have achieved good color separation. Figure 1 illustrates the analytical scheme used for analyzing three color-stained cells. The flow system is equipped with three lasers tuned to specified wavelengths and focused at points 250 μm apart on the cell stream, allowing preferential excitation and emission analysis of each dye over a preselected wavelength region and ensuring the fluorescence color resolution necessary for high sensitivity and accuracy. The three fluorescence signals and ratio signals, obtained with analog divider circuits (10), from each stained cell are collected and stored in correlated list mode in a Digital Equipment Corp. PDP11/23 computer (11) for subsequent analysis of DNA, RNA, and

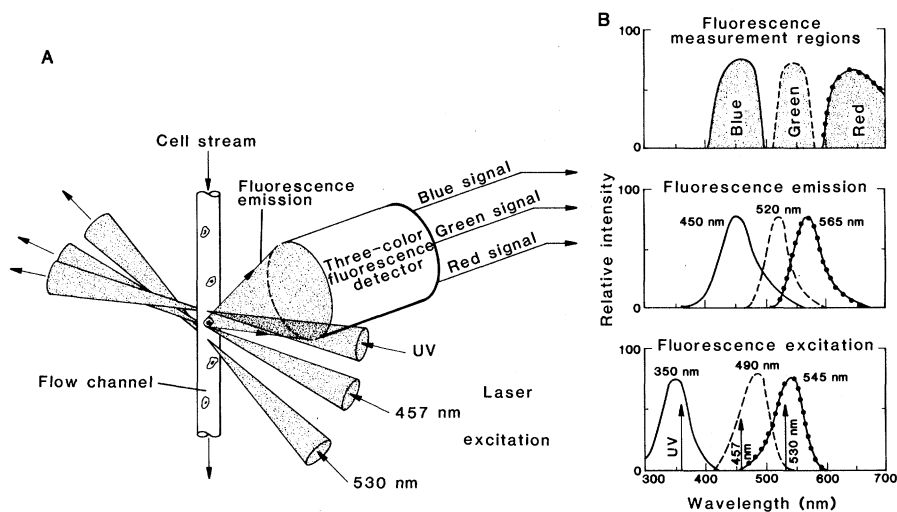


Fig. 1. (A) Three-laser excitation and fluorescence emission measurement scheme for analysis of DNA, RNA, and protein in three color-stained cells. The laser beams, tuned to the designated wavelengths, are spaced 250 μm apart. Excitation and emission analysis are thus performed preferentially for each dye at a different point on the cell stream. Measurements are correlated on a cell-to-cell basis. The three-color fluorescence detector consists of colored glass and dichroic color separating filters for measuring blue (400 to 500 nm), green (515 to 575 nm), and red (>580 nm) fluorescence emission from cells. Fluorescence signals, including ratio signals (10), are directed to signal-processing electronics for storage (correlated list mode) in a PDP11/23 computer (11) and subsequently are displayed as single-parameter frequency distribution histograms and two-parameter contour diagrams. (B) Fluorescence excitation and emission spectra and wavelength measurement regions for Hoechst 33342 (—), FITC (---), and PY (●). Arrows in the fluorescence excitation regions are laser beam wavelengths preselected for sequential excitation of each dye in stained cells.